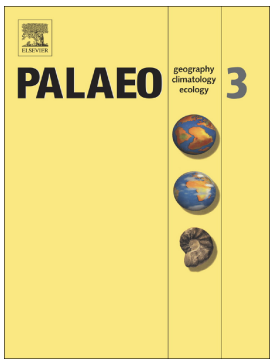

Bayesian analysis of lacustrine charcoal from Fuyun, northwestern China, records spatio-temporal variability in Altai Range fire history

Chris Gouramanis, Stephen Chua, Marie Etchebes, Yann Klinger, Xiwei Xu, Paul Tapponnier

PII: S0031-0182(26)00392-5

DOI: https://doi.org/10.1016/j.palaeo.2026.113929

Reference: PALAEO 113929

To appear in: *Palaeogeography, Palaeoclimatology, Palaeoecology*

Received date: 8 June 2025

Revised date: 8 May 2026

Accepted date: 23 May 2026

Please cite this article as: C. Gouramanis, S. Chua, M. Etchebes, et al., Bayesian analysis of lacustrine charcoal from Fuyun, northwestern China, records spatio-temporal variability in Altai Range fire history, *Palaeogeography, Palaeoclimatology, Palaeoecology* (2024), https://doi.org/10.1016/j.palaeo.2026.113929

Bayesian analysis of lacustrine charcoal from Fuyun, northwestern China, records spatio-temporal variability in Altai Range fire history

Chris Gouramanis[1,*], Stephen Chua[2,3], Marie Etchebes[4], Yann Klinger[5], Xiwei Xu[6], and Paul Tapponnier[†]

[1] *Research School of Earth Sciences, Australian National University, Canberra, 2601*

[2] *Earth Observatory of Singapore, Nanyang Technological University, Singapore, 639798*

[3] *The Asian School of the Environment, Nanyang Technological University, Singapore, 639798*

[4] *ELIIS, Clapiers, France*

[5] *Université Paris Cité, Institut de Physique du Globe de Paris, CNRS, Paris, France*

[6] *School of Earth Sciences and Resources, China University of Geosciences, Beijing 100083, China*

[†] Deceased

[*]corresponding author: Chris Gouramanis

Tel : +61 406 400 417 Email : Chris.Gouramanis@anu.edu.au

ABSTRACT

Burning histories derived from charcoal preserved in sediment archives offer scope to reconstruct past climate and landscape dynamics. The fault-bounded Aksay Pond in northwestern China preserves an 80-year sediment sequence spanning 1931 to 2012 that reveals undetected punctuated fire events within the last *ca*. 1000 years. We used Bayesian inferential modelling of 24 macrocharcoals that have been directly ^{14}C Accelerated Mass Spectrometry dated to examine past phases of fire activity and compare these phases with

other fire-proxy records from the Altai Ranges. That these charcoals formed, were stored in the landscape and subsequently mobilised into the pond suggests that fires occurred at these different times. This method for examining fire histories differs from more traditional techniques and has some inherent uncertainties that are discussed. Importantly, our charcoal record does not attempt to infer severity, intensity or number of fires but identifies undetected periods of burning. Charcoal was dated to three statistically distinct phases spanning 95% highest posterior density ranges of 1170 to 1290 CE (Phase 3), 1410 to 1650 CE (Phase 2) and 1720 to 1900 CE (Phase 1) with some post-1950 CE charcoal. Bayesian modelling also demonstrates that Phase 3 does not coincide with burning histories from elsewhere in the Altai Ranges suggesting localised fires during the early to middle stages of the Medieval Climate Anomaly. Phase 2 charcoals overlap with a significant period of burning from the western Altai Range during the early stages of the Little Ice Age (LIA) indicating a larger regional environment primed for fire. Phase 3 charcoals from Aksay Pond occurs during the transition from peak LIA to Recent Warming and likely reflects regional increases in anthropogenic burning. Our Bayesian analysis of the burning periods from the Aksay Pond with other fire records from the Altai Ranges demonstrates that burning in the region is spatio-temporally heterogeneous and that further sites need investigating to capture the true history of burning from the region.Our novel approach also demonstrates the utility of short-lived sedimentary archives as alternative proxy sources for long-term fire histories in data-scarce regions.

INTRODUCTION

Asia is the most populous continent on the planet, accounting for nearly half of humanity participating in predominantly agrarian activities (Tilman et al., 2011). Hence, central Asian countries are vulnerable to climate dynamics and fluctuations (IPCC, 2021). In particular,

uncertainty in the recent climate variability across central Asia (Kazakhstan, Kyrgyzstan, Tajikistan, Turkmenistan, Uzbekistan and northwest China's Xinjiang Province) has generated significant interest, as the income and livelihoods of approximately 93 million people living in 6 million km^2 are susceptible to a changing climate (e.g. Xu et al., 2015).

The recent spate of large regionally catastrophic forest fires has led to the need for knowledge of past fire histories to understand how recent climate change has potentially increased current and future fire hazards (e.g. Abram et al., 2021; Feng et al., 2021; Marlon et al., 2008; Wang et al., 2020). An important proxy for determining past fire histories is the presence or concentration of charcoal in sedimentary depositional environments (e.g. Harrison et al., 2022; Rehn et al., 2024). Increased concentrations of charcoal are often inferred to be the product of more frequent or intense fires in a region or increased anthropogenic activity (Mooney et al., 2011; Whitlock and Larsen, 2001). A major challenge remains to distinguish between anthropogenic and natural burning (e.g. Roos et al., 2019; Roos et al., 2018).

Across large tracts of central Asia, the East Asian and Indian monsoons dominate the annual climate system extending as far north and inland as the Altai region (Fig. 1) that straddles the China, Mongolia, Kazakhstan and Russian national borders. Much research has focused on long-term climate variation (Aizen et al., 2016; Blyakharchuk et al., 2004; Hu et al., 2024; Lehmkuhl et al., 2004; Liu et al., 2008; Rhodes et al., 1996; Rudaya et al., 2020; Rudaya et al., 2009; Zhang et al., 2020; Zhang et al., 2016), short-duration climate records (e.g. Bliedtner et al., 2021; Büntgen et al., 2016; Davi et al., 2010; Davi et al., 2009; Eichler et al., 2011; Fan et al., 2021; Myglan et al., 2012; Nazarov et al., 2012; Olivier et al., 2006; Olivier et al., 2003), and high impact climate extremes (e.g. Chen et al., 2014; Chen et al., 2016;

Davi et al., 2010; Davi et al., 2009; Fan et al., 2021; Rudaya et al., 2020). A growing body of research has focused on determining the fire histories of the region (e.g. Camara-Brugger et al., 2025; Eichler et al., 2011; Li and Wang, 2020; Olivier et al., 2006; Pupysheva and Blyakharchuk, 2024; Rudaya et al., 2020).

Across the Altai region, lake sediment and annually-dated ice core records have been examined to reconstruct past fires over a range of timeframes that do not show any coherence in spatio-temporal burning pattern. The Tsambagarav Glacier ice core record, recovered from *ca.* 150 km north of Aksay Pond, preserves charcoal with an interpreted peak burning period identified at *ca.* 1600 BCE and a burning minimum between 1700 and 1960 CE (Brugger et al., 2018). This contrasts with chemical proxies (e.g., K^+ and NO_3^-) and charcoals preserved in a Belukha ice core, recovered from *ca.* 200 km northwest of Aksay Pond (Fig. 1) that shows that peak forest fire burning occurred from *ca*. 1600 to 1680 CE (Eichler et al., 2011). Eichler et al. (2011) attribute this phase of burning as following an extreme dry period from *ca*. 1540 to 1600 CE in which biomass accumulated. From *ca*. 1680 to 1940 CE, burning rates decreased despite increased anthropogenic activity in the region (Eichler et al., 2011). Possible exceptions may have occurred between *ca*. 1860 and 1870 CE, 1880 and 1900 CE, and 1910 and 1940 CE where evidence of elevated biomass burning was identified from examination of a high-resolution Belukha ice core spanning the last two centuries (Fig 1; Olivier et al., 2006). Although the spatio-temporal heterogeneity of burning in the Altai Range is both clear from the above literature and expected in light of research from other regions (e.g. Roos and Scott, 2018; Roos et al., 2019), burning in the Altai Ranges has been treated as regionally uniform in wider fire-climate relationship comparisons (Camara-Brugger et al., 2025).

In this study, we examine a charcoal-derived ^{14}C record preserved in the sediments deposited in a fault-bounded sag pond in the southern Altai Mountains (Gouramanis et al., 2025) to explore the fire history of the region. That this pond preserves charcoals that predate the formation of the pond, allows longer-term fire histories to be reconstructed from short-duration sedimentological records. In addition, we introduce a method of applying Bayesian age modelling to individual charcoal samples to potentially identify periods of past burning from multiple disparate records. The Bayesian approach described here can be applied to other spatio-temporal comparisons to explore periods of overlap or discrimination of events.

LOCATION

Aksay Pond (60m-long and 15m-wide) is a fault-bounded sag pond formed after the 11 August 1931, Mw 7.9 earthquake on the Fuyun Fault (Gouramanis et al., 2025). It is located within the Aksay Valley between the Karachingar Mountain and the eastern Altai Range in northwestern China (Fig. 1). Aksay Pond contains approximately 2.5 m of coarse gravel and sand colluvial fan sediments in the north and fining upward packages of fine sand to mud that were periodically deposited following precipitation events (Fig. 1; Gouramanis et al., 2025). The earthquake rupture caused 1.5 m of vertical and 6 m of horizontal displacement and formed a steep, 1 to 7 meter-high, 70° northeast-dipping fault scarp that forms a shutter ridge damming the pond to the west (Gouramanis et al., 2025; Klinger et al., 2011; Liang et al., 2021).

The modern and historical climate affecting Aksay Pond is considered comparable to the weather and climate recorded from the weather station within the city of Fuyun located 40 km west of the pond in the southern Altai Range (Gouramanis et al., 2025). The climate consists of summers that are of short duration, cool and wet (average temperature of 21.3°C

and rainfall of ~20 mm), and winters are long, cold and relatively dry (average temperature of -20°C and rainfall of ~7 mm) with over 120 days of snow cover to a depth of 60 cm (Gouramanis et al., 2025; Liang et al., 2008; Shi et al., 2007; Tang et al., 2013; Zhu et al., 2015).

The local vegetation is sparse, dominated by herbaceous and small shrubby taxa, such as *Juniperus* and *Ephedra* spp. (Huang et al., 2018). Historically, the southern Altai Range in the vicinity of Aksay Pond and Karaxingar region has been largely utilised by nomadic people over the last several millennia (Chlachula, 2018), with little direct evidence of settlement or extensive usage.

METHODS

Two 20 m-long, 3 m-deep trenches were excavated across the northern (Trench A) and southern (Trench B) tips of the Aksay Pond perpendicular to the fault-trace (Fig. 1). The sedimentology, chronology and geomorphology of the sag pond and trenches are described in Gouramanis et al. (2025).

Across the four faces of the two trenches, all observed charcoal/wood/plant fragments that were greater than *ca*. 0.5 cm in diameter were excavated and stored in plastic zip lock bags before shipment and analysis at the Scottish Universities Environmental Research Centre (SUERC) for ^{14}C Accelerated Mass Spectrometry (AMS) radiocarbon dating. The samples were collected and their stratigraphic positioning recorded. After ^{14}C, ^{210}Pb and ^{137}Cs, sedimentology and stratigraphic analysis, it was determined that the pond sediments all accumulated after the 1931 earthquake (see Gouramanis et al., 2025 for more details). Of the

69 samples originally collected and analysed for ^{14}C analysis, 32 yielded sufficient carbon for robust measurement (Gouramanis et al., 2025). Of these, eight were not conclusively charcoal (diagenetically altered wood and unaltered wood fragments). Only the 24 charcoal analyses from burnt wood are used and reported in this study (Table 1). No further assessment of the anthracological characteristics were performed prior to ^{14}C analysis. Successful ^{14}C AMS dates, were randomly distributed through the stratigraphic section, and no discernible spatial or depth-related bias exists with respect to the unsuccessful ^{14}C samples. Despite the inherent limitations of this site (Gouramanis et al., 2025) and that further charcoal collection is unfeasible,we maintain that this dataset remains a representative characterization of the pond's depositional history.

The ^{14}C AMS dates were calibrated using the *ChronoModel v3* (Lanos and Dufresne, 2024). Modern (post-1950) post-bomb fractionated carbon ($F^{14}C$) results were calibrated using the Northern Hemisphere Zone 1 (Bomb21NH1) (Hua et al., 2021; Reimer et al., 2020), to obtain accurate dates on the post-1950 material. Pre-bomb ^{14}C dates were calibrated using IntCal20 northern hemisphere calibraton curve (Reimer et al., 2020). *ChronoModel* utilises Bayesian statistical inference and generates three parallel Markov Chain Monte Carlo (MCMC) simulations to infer the marginal posterior distributions of measured ages and associated errors and calculate summary statistics assuming a fixed posterior probability (here 95%) (Lanos and Philippe, 2017; Lanos and Philippe, 2018). For each chain within *ChronoModel*, we used the default settings of 1,000 burn-in iterations, 200 Max batches, 100 iterations per batch for 100,000 iterations, which were then thinned at an interval of 10 and a 0.99 mixing level (Lanos and Dufresne, 2024).

An initial plot of the calibrated age ranges suggested that there were likely different phases of burning recorded within the Aksay Pond sediments (Fig. 2). From this, we conducted several bayesian modelling iterations to identify the most likely phases (collection of dates that may correspond to a particular period of burning) of charcoal dates in *ChronoModel*. We then modelled the data to test that these phases were statistically real using the *ArchaeoPhases* (Philippe and Vibet, 2020) and *coda* (Plummer et al., 2006) packages in R. These packages examine the raw subsampled MCMC output on the marginal posterior distributions from *ChronoModel* and apply a suite of analytical tools to test the validity and structure of the MCMC iterations to determine whether sufficient MCMC convergence had occurred in the Bayesian modelling. From these iterations, we identified three phases, with Phase 3 containing the three $F^{14}C$ dates and 16 ^{14}C dates. Phase 2 and Phase 1 contained two and three ^{14}C dates, respectively (Fig. 2). Convergence was tested through the Gelman-Rubin criterion (GRc), the Geweke criterion (Gc), analysis of traceplots, examination of autocorrelation and the effective sample size (ESS) (Philippe and Vibet, 2020). For each phase, we determined the 95% highest posterior density (HPD) interval, which is the interval of time in which the true date is 95% likely to occur and most suitable for multi-modal posterior densities (Philippe and Vibet, 2020). We also test for potential gaps between the phases that may suggest hiatuses in the Aksay Pond charcoal record. These gaps are defined as the longest time span between the end-date of the older phase and the start-date of the younger phase (Philippe and Vibet, 2020).

We used identical Bayesian methods to test whether the phases of burning we identify at Aksay Pond correspond to burning phases recorded elsewhere in the Altai Ranges. To do this we re-ran our analyses but included five additional phases corresponding to three burning peaks identified by (Peak 1 = 1910-1940 CE, Peak 2 = 1880-1900 CE and Peak 3 = 1860 to

1870), and the 1600 to 1680 CE burning peak and 1700 to 2000 CE burning minima identified by Eichler et al. (2011). The Olivier et al. (2006) burning phases were determined from successive 10-year binned ice-core data, whereas the Eichler et al. (2011) geochemical proxy burning peak phase and minima were determined from ice core layer counting. Due to the lack of error associated with the start and end dates of these phases, the phases are considered uniformly distributed with start and end dates as determined by Olivier et al. (2006) and Eichler et al. (2011). We also explore whether gaps/hiatuses occurred between these and the Aksay Pond burning phases.

RESULTS

Sediments and stratigraphy

Five sedimentary facies are identified within the Aksay Pond (Fig 1D,F; Gouramanis et al., 2025). The base of the Aksay Pond consists of angular rock clasts in a silty clay matrix formed as a weathering profile of the Late Devonian volcanics of the Altai Mountains (Facies A). Overlying Facies A is a matrix-supported, brown/black muddy organic-rich layer reflective of the soils of the mountain slope (Facies B). Sufficient accommodation space for lacustrine sedimentation did not occur until after the 1931 earthquake. The lacustrine sediments within the pond consist of 11 well-preserved fining-upward sequences comprising gravelly to fine sandy layers in the north which become fine sandy to muddy layers in the south where distal sheet-flooded sediments have been deposited subaqueously (Facies D). The southern sedimentary sequence was dated using ^{210}Pb and ^{137}Cs, and the sediments were all deposited after 1963 (Gouramanis et al., 2025). Within the lacustrine sediments, three cobble and boulder-sized wedges are interpreted as slumped material from the fault scarp that may coincide with high precipitation events or small localised earthquakes (Facies C). In the

northern part of Aksay Pond is a sequence of upward-fining gravel to sand layers formed from wet debris and apron flows from a nearby colluvial fan (Facies E).

^{14}C Chronology

We obtained 32 ^{14}C AMS dates from Aksay Pond's trench walls. Of these, 24 high-quality dates were obtained from discrete charcoal fragments and eight dates from wood and plant fragments samples (Supp. Info Table). As our purpose is to examine fire histories, the wood and plant samples will not be discussed further.

Twelve charcoal samples were collected from within the buried palaeosol (Facies B) have 95% HDP ages ranging from 1050 to 1270 CE to 1690 to 1920 CE (Table 1, Fig. 1). Facies C contained three dated charcoals, one from a basal slump (Facies C1) spanning from 1670 to after 1950 CE, and two F^{14}C dates spanning 1959-1985 CE and 1970-1972 from two gravelly slumps (Facies C2) contained within the upward fining lacustrine sediments (Facies D; Fig. 1; Table 1; Gouramanis et al., 2025). Facies D contained one F^{14}C and eight ^{14}C charcoal dates spanning 1230 to 1380 to 1959 to 1989 CE (Table 1, Fig. 1). That the large spread of dates across the various stratigraphic facies, and that the dates have no correlation with sediment depth (Table 1), indicates that most of the charcoal pre-dated the formation of the pond and that most of the charcoal existed in the landscape prior to remobilisation and deposition in the pond (Gouramanis et al., 2025).

Bayesian Modelling of Aksay Pond Charcoal Phases

We identify three phases of burning from Aksay Pond charcoal (Fig. 2) with phases 1 and 2 having three and two ^{14}C dates, respectively, and Phase 3 constituting the largest group with 19 ^{14}C dates. We determine that Phase 3 constitutes both $F^{14}C$ and ^{14}C charcoal dates as calibrating the raw dates resulted in 12 ^{14}C dates being artificially stopped at 0 cal. yr. BP and most likely extending into the post-1950 period and overlapping with the $F^{14}C$ dates (Table 2; Fig. 2).

We tried different parametrization in our Bayesian modelling of the ^{14}C charcoal dates to test the robustness of the three separate phases. The initial Bayesian modelling resulted in poor MCMC convergence due to strong autocorrelation (>0.9 over 30 iterations) between the three $F^{14}C$ dates (Supp. Info. Fig. 1). We removed the $F^{14}C$ dates from further analysis, resulting in the autocorrelation decreasing to 0 after the first iteration (Supp. Info. Fig. 2) and rapid convergence in the MCMCs as determined by the excellent GRc (Potential scale reduction factors = 1), excellent Gc (Chain 1 = 0.2656 , Chain 2 = -0.3595, Chain 3 = 0.3207; all of which are $Gc<<|2|$), and excellent ESS values (Phase 1 = 19,235, Phase 2 = 17,322 and Phase 3 = 4,062). The 95% HDI derived from the Bayesian modelling confirms the visual inspection that phases 1, 2 and 3 are distinct groupings and that there are statistically significant time periods between phases 1 and 2 (131 years) and phases 2 and 3 (78 years) (Table 2 and Fig. 3).

Bayesian Modelling Comparison of Aksay Pond Charcoal Phases with Other Altai Studies

Reanalysis of the Aksay Pond phases with peak burning periods identified by Olivier et al. (2006) and Eichler et al. (2011) resulted in autocorrelation between phases decreasing to 0 within 10 iterations, and rapid convergence in the MCMCs as determined by the excellent

GRc (Potential scale reduction factors = 1), excellent Gc (Chain 1 = -0.1434 , Chain 2 = 1.63, Chain 3 = -0.1739; all of which are Gc<<|2|), and excellent ESS values (Olivier Peak 1 = 28,446, Phase 3 = 3,854, Olivier Peak 2 = 31,241, Olivier Peak 3 = 32,379, Eichler Minimum = 26,440, Eichler Peak = 29,458, Phase 2 = 18,022, and Phase 1 = 18,612). The reanalysis confirms the findings of the Aksay Pond-only ^{14}C Bayesian modelling, albeit with subtly different phase duration and gap analyses start, end and duration dates (c.f. Table 2 and Table 3). These differences are due to the separate modelling implemented for the 'Aksay Pond-only' analyses and the 'Aksay Pond and other studies' analyses'.

The 95% HDI derived from the 'Aksay Pond and other studies' Bayesian modelling analyses clearly shows that Phase 3 overlaps (i.e. no gap) between the three Olivier peaks and the Eichler Minima and Eichler Peak, Phase 2 overlaps with the Eichler Minimum and Eichler Peak (Table 2 and Table 3). Only Phase 1 has a significant gap between the Eichler Minimum (256 years) and Eichler Peak (263 years) (Table 2 and Table 3).

DISCUSSION

Bias in charcoal records

Macrocharcoals and/or microcharcoals are commonly counted to reconstruct fire histories from sedimentary archives (e.g. Conedera et al., 2009; Vachula et al., 2018). These studies also require robust chronologies to establish the time of charcoal deposition, either through directly dating the charcoal horizons or extrapolating ages from bracketing dates (e.g. Schmid et al., 2018; Turner et al., 2008). The ages of the charcoal horizons are then inferred to reflect the time of the fire. Assumptions exist whether charcoal fragments originated from a single fire or multiple fires, or whether the charcoal have been remobilised after storage in the

landscape or to what effect the charcoal had undergone further mechanical or chemical breakdown before deposition in a sedimentary environment (e.g. Mergelov et al., 2025; Ohlson et al., 2013; Ryan et al., 2025; Ryan et al., 2024). At Aksay Pond, we directly dated the individual charcoals within the sedimentary sequence and these define when each individual charcoal was formed.

As our Aksay Pond record spans 1931 to 2012 CE with likely periods of rapid sediment accumulation, quiescence and deflation (Gouramanis et al., 2025), the presence of older charcoals (Table 1, Fig. 2) *implies* that the charcoals were stored in the landscape prior to mobilisation and deposition. Nine charcoals are definitively older than the 1931 CE pond-initiation date (at the upper limit of the 95% HPD – Table 1) and so are direct evidence of fires before the pond formed. That these nine are found throughout the sedimentary sequence and in the underlying soil indicates that the charcoal has been stored within the palaeosol, subsequently mobilised and redeposited into the pond at different times after 1931 CE. In addition, five other charcoals scattered throughout the palaeosol and sedimentary sequence have their upper 95% HPD range indeterminable as these upper bounds post-date the 1950 pre-bomb ^{14}C calibration (Table 1) (Reimer et al., 2020). The mean ages for these five charcoals range from the mid to late-18th Century to very early 19th Century CE, suggesting that they were likely formed prior to the initiation of the pond. Seven more charcoals have their upper 95% HPD range between the 1931 CE pond initiation and the 1950 pre-bomb ^{14}C calibration cut off, but have mean calculated ages clustered between 1809 and 1819 CE, suggesting that they were likely remobilised into the Aksay Pond sedimentary environment well after the fire event.

Of note are the relatively large 95% HPD age ranges (300 to 400 years) of 16 charcoal dates that span the prolonged radiocarbon plateau (e.g. Hua, 2009) from the mid-17th Century to the early 20th Centuy CE. Based on those ranges, we cannot ascribe these to a particular or multiple fire events. However, given the range of $\delta^{13}C$ values of the charcoal (-20.7 to -28.1‰), it is likely that different trees and possibly multiple species, growing under different climatic conditions, were burnt to produce the charcoals in Phase 3 (Table 1). For example, individuals of *Pinus koraiensis*, *Quercus mongolica* and *Larix gmelinii* from northeastern China showed between 1 and 3‰ differences between the $\delta^{13}C$ composition of their leaves, branches, trunks and roots (Li and Zhu, 2011). Even acknowledging this narrow intra-specimen $\delta^{13}C$ range, we cannot discount that a single fire event resulted in the charcoal ages as woody plant material may have accumulated in the landscape prior to burning. In future, applying techniques, such as Attenuated Total Reflectance Fourier Transform Infrared spectroscopy (Ryan et al., 2025; Ryan et al., 2024), Raman spectroscopy (Mergelov et al., 2025) and charcoal reflectance (e.g. Belcher et al., 2021; Belcher et al., 2018; Roos and Scott, 2018), offers opportunities to test the severity and intensity of fires from individual charcoal horizons. Similarly, more detailed anthracological or botanical data, such as wood curvature, observable rings or other species-specific structural information on each charcoal fragment may have shed light on the history of the wood and charcoal that was eventually sampled (e.g. Kabukcu and Chabal, 2021; Théry-Parisot et al.; Walsh et al., 2024).

Importantly, only three charcoals from Aksay Pond are defnitively younger than the 1931 CE pond-initiation date (Table 1). Two of the charcoals were recovered from 100 cm depth in Trench B South Face (Fig. 1d, Table 1), and although their mean ages differ (FU12-C14-51 = 1988 CE and FU12-C14-94 = 1971 CE), their 95% HDP ranges overlap (FU12-C14-51 =

1959 to 1989 CE and FU12-C14-94 = 1970 to 1972 CE) it is not possible to determine whether they originate from the same burning event or different burning events.

We acknolwedge that finer charcoals may be present in our area, but these were not collected as they could not be individually dated. Similarly, given the short duration of primary deposition (*ca*. 80 years) and that all of the pre-1930's charcoal must be remobilised, it is not possible to derive viable events or burning periods from finer charcoals. We recognise that finer charcoals may have formed at different times to the macrocharcoals, but cannot validate this contention. As our results show, charcoals from the same or similar horizons (Table 1) can produce vastly different ages due to the differential redistribution of the charcoals during pond sedimentation. As such, pooling of small charcoal samples is not appropriate for ^{14}C dating at our site. This limitation exists here as well as in other fire reconstruction records where macrocharcoals are analysed or microcharcoals are pooled (Carcaillet, 2001; Graves et al., 2019). Where other studies count macrocharcoals and/or microcharcoals to derive burning histories, these charcoals are typically not ^{14}C dated, are undatable due to their size, composition, morphotype and/or fragility, or only a small subset are ^{14}C dated (e.g. Eckmeier et al., 2016; Enache and Cumming, 2007; Higuera et al., 2010). Of note, when charcoals are ^{14}C dated, other undated charcoals from the same or adjacent horizons are considered coeval despite the knowledge that charcoals can be stored and later remobilised (e.g. Blong et al., 2023; Pompeani et al., 2020; Wood et al., 2023). The issues associated with dating charcoals versus size and number of charcoals used/counted in fire reconstructions remains an outstanding issue in the fire reconstruction literature (Harrison et al., 2022; Wood et al., 2023). That macrocharcoals can be transported long distances is well established (e.g. Benedict, 2002; Tinner et al., 2006) and macrocharcoal presence within a depositional record are not necessarily a consequence of local fires. The analysis of macrocharcoals here, does

not disqualify our analysis that macrocharcoal formation has occurred at different times to other studies in the region and strengthens our hypothesis for the spatial heterogeneity of fire across the Altai Range (as discussed below).

Fire and climate history from Aksay Pond

Based on the 95% HDP age ranges of the ^{14}C AMS charcoal dates from Aksay Pond and the Bayesian hiatus modelling there were three discrete periods where burned vegetation was stored in the soil and sediment record near the pond (Fig. 2; Table 1). The earliest period of burning (Phase 1) is recorded in three macrocharcoal dates with 95% HDP age range spanning *ca.* 1170 to 1290 CE. An intermediate period of burning (Phase 2) is recorded in two macrocharcoal dates spanning *ca*. 1410 and 1650 CE (95% HPD range). The latest period (Phase 3) is captured by 16 dates (after removal of the three F^{14}C dates) that have a 95% HPD range spanning *ca*. 1720 to 1900 CE. From a climatic perspective, based on low resolution palaeoclimate records, no consensus has emerged about climatic changes in the region through the Late Holocene. Some studies have proposed that climatic conditions remained stable with no significant change (e.g. Blyakharchuk et al., 2004), or that the region became drier (e.g. Bliedtner et al., 2021; Brugger et al., 2018; Liu et al., 2008; Rhodes et al., 1996; Rudaya et al., 2009; Zhang et al., 2016) or, conversely, became wetter (e.g. Hu et al., 2024). In addition, several of these records suggest that human landscape modification intensified in the Late Holocene (e.g. Brugger et al., 2018; Rudaya et al., 2009; Schlütz and Lehmkuhl, 2006). Camara-Brugger et al. (2025) suggested that weakening monsoonal activity resulted in drying and subsequent changes to vegetation that decreased fire activity in the late Holocene.

Higher resolution climate records from tree rings, ice cores and lake sediment archives resolve some of these climate discrepancies. Charcoal from Phase 1 from the Aksay Pond coincides with the warm and dry Medieval Climate Anomaly (MCA, *ca.* 1090 to 1430 CE; Fig. 2B) in the region (Aizen et al., 2016; Büntgen et al., 2016; Li et al., 2017; Myglan et al., 2012). Nazarov et al. (2012) note an upper tree line decline between *ca.*1206 to 1256 CE in the central and eastern Altai ranges suggesting a significant decrease in temperature. Eichler et al. (2011) did not measure chemical fire proxies (K^+ or NO_3^-) or charcoal from their Belukha Glacier record from this period, as their record only extended back to *ca*. 1250 CE (Fig. 2C). Aizen et al. (2016)'s West Belukha Plateau ice record extends back to *ca*. 10,000 BCE and does not preserve an identifiable burning history. Brugger et al. (2018)'s Tsambagarav Glacier charcoal record identified a peak period of burning at *ca*. 1600 BCE, well before our record begins. Notably, our comparison of the Phase 1 burning from Aksay Pond and other burning reconstructions does not show any significant overlap (Fig. 4; Table 3). The lack of coherency in the regional records suggests that the burning preserved in Aksay Pond from this period may have originated from localised fires. Importantly, and like other parts of the world, it is most likely that palaeo-fire records from the Altai region will be spatially and temporally incoherent making a unified fire history challenging to decipher (e.g. Roos et al., 2019; Roos et al., 2018).

The Phase 2 Aksay Pond charcoal occurs in the early to middle stages of the Little Ice Age (spanning *ca*. 1400 to 1870 CE) although it does not coincide with significant low temperatures (Aizen et al., 2016; Büntgen et al., 2016; Li et al., 2017). This contrasts with Nazarov et al. (2012) who record significant decline in upper tree limit between *ca.* 1445 to 1501 CE. Fan et al. (2021) demonstrated from Yileimu Lake that from *ca*. 1586 to 1620 CE was a period of extreme drought. Fires may have occurred during this dry phase but were not

explored in the Yileimu Lake record. However, Eichler et al. (2011) identified *ca*. 1600 to 1680 CE as a major period of burning following an expansive dry phase from *ca*. 1540 to 1600 CE from the southern Siberian Altai (Fig. 2C). That Phase 2 Aksay Pond charcoals significantly overlap with the Eichler et al. (2011) burning peak (Fig. 4; Table 3) may suggest a more widespread period of burning across the Altai Range The Aksay Pond macrocharcoal dated to this period indicates that macrocharcoal was either transported to the southern Altai Range or that fire conditions occurred locally. Given the local geomorphology and the size of the macrocharcoal fragments extracted from the trench walls, there is a much higher likelihood that the fires occurred locally, likely proximal to the sag pond.

The charcoal in Phase 3 from the Aksay Pond spans the transition from the peak of the LIA to the period of Recent Warming (RW; after 1940 CE) (Aizen et al., 2016; Büntgen et al., 2016; Eichler et al., 2011; Li et al., 2017). Nazarov et al. (2012) recognised significant tree mortality between *ca.* 1642 and 1736 CE caused by temperature decline and glacial advancement in the southern Russian Altai region. Of note, this timing of tree decline differs from Eichler et al. (2011)'s finding that vegetation decline occurred between *ca*. 1540 and 1600 CE and that peak burning occurred between *ca*. 1600 and 1680 CE in the same region. Davi et al. (2009) identified an extreme wet phase from western Mongolian tree rings from *ca.* 1739 to 1746 CE, and extreme dry periods from *ca*. 1755 to 1761 CE and *ca*. 1882 to 1886 CE. Chen et al. (2014) identified numerous short-lived wet and dry phases in their analyses of tree rings from northern China that are similar to those recorded in Davi et al. (2009). In contrast, Fan et al. (2021) suggested the period from *ca.* 1620 to 1835 CE was characterised by increased summer warming and winter snowfall, and from *ca.* 1835 to 1870 CE by extreme drought. Of note, the tree ring records from near the Aksay Pond (Chen et al., 2014; Chen et al., 2016; Davi et al., 2009) and Fan et al. (2021)'s Lake Yileimu record are

separated by only 200 km and it is surprising that the lake record differs substantially from the tree ring records. In addition, charcoal from the Tsambagarav Glacier, indicates a fire minimum from *ca*. 1700 to 1960 CE. The Aksay Pond Phase 3 charcoal overlaps with all of (Olivier et al., 2006)'s peaks (Table 3, Fig. 4). However, Xu et al. (2015) argue for localised climate variability based on modern climatic records. Büntgen et al. (2016) identified the RW period as the warmest in the 2000 year long tree ring record from the Altai region. Davi et al. (2009) suggested that *ca.* 1993 to 2003 CE was the second wettest phase in their 439 year record. Aizen et al. (2016) and Eichler et al. (2011) show that there is little biomass burning identified from their respective ice cores in the Belukha region between 1700 and 2000 CE, but note that major fires have occurred in 1915, 1974, 1991 and 2003. This contrasts with Olivier et al. (2006)'s high resolution analysis of the last 200 years of the Bekhula ice core record that indicated small fire peaks between 1860 to 1870 CE (Peak 3), 1880-1900 CE (Peak 2) and 1910-1940 CE (Peak 1), and that overlap with Phase 3 charcoals from Aksay Pond (Table 3; Fig. 4). This suggests the occurrence of localised fires, or fires that occurred east of the Belukha sites that created macrocharcoal that were subsequently transported to Aksay Pond. In addition, a slightly increased fire record is preserved in the Tsambagarav Glacier between 1960 and 2000 CE may attest to localised anthropogenic activity (Brugger et al., 2018). The large forest fires recorded from the Altai Range and Southwestern Siberia in 1921, 1974 and 1991 (e.g. Aizen et al., 2016; and references therein) and may also coincide with our later ^{14}C and $F^{14}C$ charcoal results.

CONCLUSION

The small fault-bounded Aksay Pond in the southern Altai Range in northwestern China, provides a burning history of the area. We utilised a dense analysis of macrocharcoal ^{14}C

AMS dates recovered from sediments within Aksay Pond to provide evidence of when the vegetation burned, and show that these charcoals persisted in the surrounding environment prior to transport and preservation. Bayesian modelling identified three distinct phases of burning from Aksay Pond charcoals spanning 1170 to 1290 CE (Phase 1), 1410 to 1650 CE (Phase 2) and 1720 to 1900 CE (Phase 3), with suggestion that some vegetation was burnt after 1950 CE. Using Bayesian methods, we also compared the Aksay Pond burning phases with other Altai Range burning histories and show that Phase 1 may have been localised to the Aksay Pond region as no evidence exists elsewhere from the Altai Ranges. Phase 1 also coincides with the MCA in northwestern China, suggesting a climate link to the fires. Phase 2 coincides with the LIA in northwestern China and overlaps with a burning peak derived from ice core records from the southern Siberian Altai Range, suggesting that the climate and vegetation across the Altai Ranges was primed for burning. However, further investigation is required to determine whether this fire period is both temporally and spatially contiguous. From the western Altai Mountains, fire activity had increased after 1420 CE that Rudaya et al. (2020) attribute to anthropogenic activities. We cannot attribute this increased burning trend, but more post-1410 CE charcoal dates preserved within the Aksay Pond (Phases 2 and 3) adds credence to this increased fire activity. Unfortunately, as our record preserves remobilised macrocharcoal, we cannot verify whether these charcoals came from a single or multiple events. Uniquely, our study also demonstrates that long-term fire histories can be reconstructed from short-duration lake records, and this can open up possibilities for fire reconstruction where long sedimentological records are absent. Additionally, our usage of Bayesian methods have wider applicability in the palaeoenvironmental and palaeoclimatological communities to evaluate spatio-temporal patterns of events and intervals. The high degree of climate and fire variability recorded between different proxy records from the Altai Range supports the contention that fire across the region is highly

spatially and temporally variable. Further research into this region is required to develop a coherent assessment of climate and fire histories.

ACKNOWLEDGMENTS

We thank Singapore's Ministry of Education for funding this research under Grant No: R-109-000-248-115 (C.G.). Y.K was supported by ANR-05-CATT-0006. We are indebted to two anonymous reviewers for their critical analysis of our manuscript and their valuable comments that have strengthened our findings. We also thank Prof. Mary Elliott for handling our manuscript.

References

Abram, N.J., Henley, B.J., Sen Gupta, A., Lippmann, T.J.R., Clarke, H., Dowdy, A.J., Sharples, J.J., Nolan, R.H., Zhang, T., Wooster, M.J., Wurtzel, J.B., Meissner, K.J., Pitman, A.J., Ukkola, A.M., Murphy, B.P., Tapper, N.J., Boer, M.M., 2021. Connections of climate change and variability to large and extreme forest fires in southeast Australia. Communications Earth & Environment 2.

Aizen, E.M., Aizen, V.B., Takeuchi, N., Mayewski, P.A., Grigholm, B., Joswiak, D.R., Nikitin, S.A., Fujita, K., Nakawo, M., Zapf, A., Schwikowski, M., 2016. Abrupt and moderate climate changes in the mid-latitudes of Asia during the Holocene. Journal of Glaciology 62, 411-439.

Belcher, C.M., New, S.L., Gallagher, M.R., Grosvenor, M.J., Clark, K., Skowronski, N.S., 2021. Bark charcoal reflectance may have the potential to estimate the heat delivered to tree boles by wildland fires. International Journal of Wildland Fire 30, 391-397.

Belcher, C.M., New, S.L., Santín, C., Doerr, S.H., Dewhirst, R.A., Grosvenor, M.J., Hudspith, V.A., 2018. What Can Charcoal Reflectance Tell Us About Energy Release in Wildfires and the Properties of Pyrogenic Carbon? Frontiers in Earth Science 6.

Benedict, J.B., 2002. Eolian Deposition of Forest-Fire Charcoal above Tree Limit, Colorado Front Range, U.S.A.: Potential Contamination of AMS Radiocarbon Samples. Arctic, Antarctic, and Alpine Research 34, 33-37.

Bliedtner, M., Struck, J., Strobel, P., Salazar, G., Szidat, S., Bazarradnaa, E., Lloren, R., Dubois, N., Zech, R., 2021. Late Holocene Climate Changes in the Altai Region Based on a First High-Resolution Biomarker Isotope Record From Lake Khar Nuur. Geophysical Research Letters 48.

Blong, R., Fryirs, K., Wood, R., King, F., Schneider, L., Dotte-Sarout, E., Fallon, S., Gillespie, R., Chen, Q., Esmay, R., 2023. Inherited age of floating charcoal fragments in a sand-bed stream, Macdonald River, NSW, Australia: Implications for radiocarbon dating of sediments. The Holocene 33, 1154-1159.

Blyakharchuk, T.A., Wright, H.E., Borodavko, P.S., van der Knaap, W.O., Ammann, B., 2004. Late Glacial and Holocene vegetational changes on the Ulagan high-mountain plateau, Altai Mountains, southern Siberia. Palaeogeography, Palaeoclimatology, Palaeoecology 209, 259-279.

Brugger, S.O., Gobet, E., Sigl, M., Osmont, D., Papina, T., Rudaya, N., Schwikowski, M., Tinner, W., 2018. Ice records provide new insights into climatic vulnerability of Central Asian forest and steppe communities. Global and Planetary Change 169, 188-201.
Büntgen, U., Myglan, V.S., Ljungqvist, F.C., McCormick, M., Di Cosmo, N., Sigl, M., Jungclaus, J., Wagner, S., Krusic, P.J., Esper, J., Kaplan, J.O., de Vaan, M.A.C., Luterbacher, J., Wacker, L., Tegel, W., Kirdyanov, A.V., 2016. Cooling and societal change during the Late Antique Little Ice Age from 536 to around 660 AD. Nature Geoscience 9, 231-236.
Camara-Brugger, S.O., Wanner, H., Gobet, E., Tinner, W., Schwikowski, M., 2025. Monsoon-driven teleconnections between Holocene fire activity in Central Asian and Neotropical ecosystems. Climatic Change 178.
Carcaillet, C., 2001. Are Holocene wood-charcoal fragments stratified in alpine and subalpine soils? Evidence from the Alps based on AMS ^{14}C dates. The Holocene 11, 231-242.
Chen, F., Yuan, Y.-j., Wei, W.-s., Zhang, T.-w., Shang, H.-m., Zhang, R., 2014. Precipitation reconstruction for the southern Altay Mountains (China) from tree rings of Siberian spruce, reveals recent wetting trend. Dendrochronologia 32, 266-272.
Chen, F., Yuan, Y., Davi, N., Zhang, T., 2016. Upper Irtysh River flow since AD 1500 as reconstructed by tree rings, reveals the hydroclimatic signal of inner Asia. Climatic Change 139, 651-665.
Chlachula, J., 2018. Environmental context and adaptations of prehistoric and early historical occupation in the Southern Altai (SW Siberia–East Kazakhstan). Archaeological and Anthropological Sciences 11, 2215-2236.
Conedera, M., Tinner, W., Neff, C., Meurer, M., Dickens, A.F., Krebs, P., 2009. Reconstructing past fire regimes: methods, applications, and relevance to fire management and conservation. Quaternary Science Reviews 28, 555-576.
Davi, N., Jacoby, G., Fang, K., Li, J., D'Arrigo, R., Baatarbileg, N., Robinson, D., 2010. Reconstructing drought variability for Mongolia based on a large-scale tree ring network: 1520–1993. Journal of Geophysical Research: Atmospheres 115.
Davi, N.K., Jacoby, G.C., D'Arrigo, R.D., Baatarbileg, N., Jinbao, L., Curtis, A.E., 2009. A tree-ring-based drought index reconstruction for far-western Mongolia: 1565–2004. International Journal of Climatology 29, 1508-1514.
Eckmeier, E., Van der Borg, K., Tegtmeier, U., Schmidt, M.W.I., Gerlach, R., 2016. Dating Charred Soil Organic Matter: Comparison of Radiocarbon Ages from Macrocharcoals and Chemically Separated Charcoal Carbon. Radiocarbon 51, 437-443.
Eichler, A., Tinner, W., Brütsch, S., Olivier, S., Papina, T., Schwikowski, M., 2011. An ice-core based history of Siberian forest fires since AD 1250. Quaternary Science Reviews 30, 1027-1034.
Enache, M.D., Cumming, B.F., 2007. Charcoal morphotypes in lake sediments from British Columbia (Canada): an assessment of their utility for the reconstruction of past fire and precipitation. Journal of Paleolimnology 38, 347-363.
Fan, J., Jiang, H., Shi, W., Guo, Q., Zhang, S., Wei, X., Xu, H., Liu, Y., Xue, D., Zhong, N., Huang, S., Chang, X., Shi, X., Yasen, O., Bahetihan, Y., Xiao, J., 2021. A 450-year warming and wetting climate in southern Altay inferred from a Yileimu Lake sediment core. Quaternary International 592, 37-50.
Feng, X., Merow, C., Liu, Z., Park, D.S., Roehrdanz, P.R., Maitner, B., Newman, E.A., Boyle, B.L., Lien, A., Burger, J.R., Pires, M.M., Brando, P.M., Bush, M.B., McMichael, C.N.H., Neves, D.M., Nikolopoulos, E.I., Saleska, S.R., Hannah, L., Breshears, D.D., Evans, T.P., Soto, J.R., Ernst, K.C., Enquist, B.J., 2021. How deregulation, drought and increasing fire impact Amazonian biodiversity. Nature 597, 516-521.
Gouramanis, C., Chua, S., Etchebes, M., Klinger, Y., Xu, X., Mingxing, G., Switzer, A.D., Hancock, G., Tapponnier, P., 2025. Episodic rainfall events characterise complex sediment deposition in a fault-bounded sag pond in Northwest China. Geomorphology 470.
Graves, B.P., Ralph, T.J., Hesse, P.P., Westaway, K.E., Kobayashi, T., Gadd, P.S., Mazumder, D., 2019. Macro-charcoal accumulation in floodplain wetlands: Problems and prospects for reconstruction of fire regimes and environmental conditions. PLoS One 14, e0224011.

Harrison, S.P., Villegas-Diaz, R., Cruz-Silva, E., Gallagher, D., Kesner, D., Lincoln, P., Shen, Y., Sweeney, L., Colombaroli, D., Ali, A., Barhoumi, C., Bergeron, Y., Blyakharchuk, T., Bobek, P., Bradshaw, R., Clear, J.L., Czerwiński, S., Daniau, A.-L., Dodson, J., Edwards, K.J., Edwards, M.E., Feurdean, A., Foster, D., Gajewski, K., Gałka, M., Garneau, M., Giesecke, T., Gil Romera, G., Girardin, M.P., Hoefer, D., Huang, K., Inoue, J., Jamrichová, E., Jasiunas, N., Jiang, W., Jiménez-Moreno, G., Karpińska-Kołaczek, M., Kołaczek, P., Kuosmanen, N., Lamentowicz, M., Lavoie, M., Li, F., Li, J., Lisitsyna, O., López-Sáez, J.A., Luelmo-Lautenschlaeger, R., Magnan, G., Magyari, E.K., Maksims, A., Marcisz, K., Marinova, E., Marlon, J., Mensing, S., Miroslaw-Grabowska, J., Oswald, W., Pérez-Díaz, S., Pérez-Obiol, R., Piilo, S., Poska, A., Qin, X., Remy, C.C., Richard, P.J.H., Salonen, S., Sasaki, N., Schneider, H., Shotyk, W., Stancikaite, M., Šteinberga, D., Stivrins, N., Takahara, H., Tan, Z., Trasune, L., Umbanhowar, C.E., Väliranta, M., Vassiljev, J., Xiao, X., Xu, Q., Xu, X., Zawisza, E., Zhao, Y., Zhou, Z., Paillard, J., 2022. The Reading Palaeofire Database: an expanded global resource to document changes in fire regimes from sedimentary charcoal records. Earth System Science Data 14, 1109-1124.

Higuera, P.E., Gavin, D.G., Bartlein, P.J., Hallet, D.J., 2010 Peak detection in sediment–charcoal records Impacts of alternative data analysis methods on fire history interpretations. International Journal of Wildland Fire 19, 996–1014.

Hu, Y., Huang, X., Demberel, O., Zhang, J., Xiang, L., Gundegmaa, V., Huang, C., Zheng, M., Zhang, J., Qiang, M., Xiao, J., Chen, F., 2024. Quantitative reconstruction of precipitation changes in the Mongolian Altai Mountains since 13.7 ka. Catena 234.

Hua, Q., 2009. Radiocarbon: A chronological tool for the recent past. Quaternary Geochronology 4, 378-390.

Hua, Q., Turnbull, J.C., Santos, G.M., Rakowski, A.Z., Ancapichún, S., De Pol-Holz, R., Hammer, S., Lehman, S.J., Levin, I., Miller, J.B., Palmer, J.G., Turney, C.S.M., 2021. Atmospheric Radiocarbon for the Period 1950–2019. Radiocarbon 64, 723-745.

Huang, X., Peng, W., Rudaya, N., Grimm, E.C., Chen, X., Cao, X., Zhang, J., Pan, X., Liu, S., Chen, C., Chen, F., 2018. Holocene Vegetation and Climate Dynamics in the Altai Mountains and Surrounding Areas. Geophysical Research Letters 45, 6628-6636.

IPCC, 2021. Climate Change 2021: The Physical Science Basis. Contribution of Working Group I to the Sixth Assessment Report of the Intergovernmental Panel on Climate Change, in: Masson-Delmotte, V., Zhai, P., Pirani, A., Connors, S.L., Péan, C., Berger, S., Caud, N., Chen, Y., Goldfarb, L., Gomis, M.I., Huang, M., Leitzell, K., Lonnoy, E., Matthews, J.B.R., Maycock, T.K., Waterfield, T., Yelekçi, O., Yu, R., Zhou, B. (Eds.). Cambridge University Press, Cambridge, UK, p. 3949.

Kabukcu, C., Chabal, L., 2021. Sampling and quantitative analysis methods in anthracology from archaeological contexts: Achievements and prospects. Quaternary International 593-594, 6-18.

Klinger, Y., Etchebes, M., Tapponnier, P., Narteau, C., 2011. Characteristic slip for five great earthquakes along the Fuyun fault in China. Nature Geoscience 4, 389-392.

Lanos, P., Dufresne, P., 2024. ChronoModel version 3 User Manual, 3 ed.

Lanos, P., Philippe, A., 2017. Hierarchical Bayesian modeling for combining dates in archeological context. Journal de la Société Française de Statistique 158, 72–88.

Lanos, P., Philippe, A., 2018. Event date model: a robust Bayesian tool for chronology building. Communications for Statistical Applications and Methods 25, 131-157.

Lehmkuhl, F., Klinge, M., Stauch, G., 2004. The extent of Late Pleistocene glaciations in the Altai and Khangai Mountains, in: Ehlers, J., Gibbard, P.L. (Eds.), Quaternary Glaciations - Extent and Chronology, Part III, pp. 243-254.

Li, J., Wang, N., 2020. Holocene Grassland Fire Dynamics and Forcing Factors in Continental Interior of China. Geophysical Research Letters 47.

Li, M., Zhu, J., 2011. Variation of $\delta^{13}C$ of wood and foliage with canopy height differs between evergreen and deciduous species in a temperate forest. Plant Ecology 212, 543-551.

Li, Y., Qiang, M., Zhang, J., Huang, X., Zhou, A., Chen, J., Wang, G., Zhao, Y., 2017. Hydroclimatic changes over the past 900 years documented by the sediments of Tiewaike Lake, Altai Mountains, Northwestern China. Quaternary International 452, 91-101.

Liang, T., Huang, X., Wu, C., Liu, X., Li, W., Guo, Z., Ren, J., 2008. An application of MODIS data to snow cover monitoring in a pastoral area: A case study in Northern Xinjiang, China. Remote Sensing of Environment 112, 1514-1526.
Liang, Z., Wei, Z., Sun, W., Zhuang, Q., Zielke, O., 2021. Surface Slip Distribution and Earthquake Rupture Model of the Fuyun Fault, China, Based on High-Resolution Topographic Data. Lithosphere 2021.
Liu, X., Herzschuh, U., Shen, J., Jiang, Q., Xiao, X., 2008. Holocene environmental and climatic changes inferred from Wulungu Lake in northern Xinjiang, China. Quaternary Research 70, 412-425.
Marlon, J.R., Bartlein, P.J., Carcaillet, C., Gavin, D.G., Harrison, S.P., Higuera, P.E., Joos, F., Power, M.J., Prentice, I.C., 2008. Climate and human influences on global biomass burning over the past two millennia. Nature Geoscience 1, 697-702.
Mergelov, N., Zazovskaya, E., Onishchenko, N., Petrov, D., Dolgikh, A., Turchinskaya, S., Dobryansky, A., Garankina, E., Shorkunov, I., 2025. The memory of soil charcoal assessed by Raman spectroscopy: A continuum of molecular signatures structured by production conditions and ageing (case study on boreal soils). Catena 255.
Mooney, S.D., Harrison, S.P., Bartlein, P.J., Daniau, A.L., Stevenson, J., Brownlie, K.C., Buckman, S., Cupper, M., Luly, J., Black, M., Colhoun, E., D'Costa, D., Dodson, J., Haberle, S., Hope, G.S., Kershaw, P., Kenyon, C., McKenzie, M., Williams, N., 2011. Late Quaternary fire regimes of Australasia. Quaternary Science Reviews 30, 28-46.
Myglan, V.S., Zharnikova, O.A., Malysheva, N.V., Gerasimova, O.V., Vaganov, E.A., Sidorov, O.V., 2012. Constructing the tree-ring chronology and reconstructing summertime air temperatures in southern Altai for the last 1500 years. Geography and Natural Resources 33, 200-207.
Nazarov, A.N., Solomina, O.N., Myglan, V.S., 2012. Variations of the tree line and glaciers in the Central and Eastern Altai regions in the Holocene. Doklady Earth Sciences 444, 787-790.
Ohlson, M., Kasin, I., Wist, A.N., Bjune, A.E., 2013. Size and spatial structure of the soil and lacustrine charcoal pool across a boreal forest watershed. Quaternary Research 80, 417-424.
Olivier, S., Blaser, C., Brütsch, S., Frolova, N., Gäggeler, H.W., Henderson, K.A., Palmer, A.S., Papina, T., Schwikowski, M., 2006. Temporal variations of mineral dust, biogenic tracers, and anthropogenic species during the past two centuries from Belukha ice core, Siberian Altai. Journal of Geophysical Research: Atmospheres 111.
Olivier, S., Schwikowski, M., Brütsch, S., Eyrikh, S., Gäggeler, H.W., Lüthi, M., Papina, T., Saurer, M., Schotterer, U., Tobler, L., Vogel, E., 2003. Glaciochemical investigation of an ice core from Belukha glacier, Siberian Altai. Geophysical Research Letters 30.
Philippe, A., Vibet, M.-A., 2020. Analysis of Archaeological Phases Using the R Package ArchaeoPhases. Journal of Statistical Software 93.
Plummer, M., Best, N., Cowles, K., Vines, K., 2006. CODA: Convergence Diagnosis and Output Analysis for MCMC. R News 6, 7-11.
Pompeani, D.P., McLauchlan, K.K., Chileen, B.V., Calder, W.J., Shuman, B.N., Higuera, P.E., 2020. The biogeochemical consequences of late Holocene wildfires in three subalpine lakes from northern Colorado. Quaternary Science Reviews 236.
Pupysheva, M.A., Blyakharchuk, T.A., 2024. The influence of palaeo-fire activity on the dynamics of vegetation cover in the piedmont of Northern Altai for the past 16000 years. Limnology and Freshwater Biology, 588-593.
Rehn, E., Cadd, H., Mooney, S., Cohen, T.J., Munack, H., Codilean, A.T., Adeleye, M., Beck, K.K., Constantine Iv, M., Gouramanis, C., Hanson, J.M., Jones, P.J., Kershaw, A.P., Mackenzie, L., Maisie, M., Mariani, M., Mately, K., McWethy, D., Mills, K., Moss, P., Patton, N.R., Rowe, C., Stevenson, J., Tibby, J., Wilmshurst, J., 2024. The SahulCHAR Collection: A Palaeofire Database for Australia, New Guinea, and New Zealand. Earth System Science Data.
Reimer, P.J., Austin, W.E.N., Bard, E., Bayliss, A., Blackwell, P.G., Bronk Ramsey, C., Butzin, M., Cheng, H., Edwards, R.L., Friedrich, M., Grootes, P.M., Guilderson, T.P., Hajdas, I., Heaton, T.J., Hogg, A.G., Hughen, K.A., Kromer, B., Manning, S.W., Muscheler, R., Palmer, J.G., Pearson, C., van der Plicht, J.,

Reimer, R.W., Richards, D.A., Scott, E.M., Southon, J.R., Turney, C.S.M., Wacker, L., Adolphi, F., Büntgen, U., Capano, M., Fahrni, S.M., Fogtmann-Schulz, A., Friedrich, R., Köhler, P., Kudsk, S., Miyake, F., Olsen, J., Reinig, F., Sakamoto, M., Sookdeo, A., Talamo, S., 2020. The IntCal20 Northern Hemisphere Radiocarbon Age Calibration Curve (0–55 cal kBP). Radiocarbon 62, 725-757.
Rhodes, T.E., Gasse, F., Ruifen, L., Fontes, J.-C., Keqin, W., Bertrand, P., Gibert, E., Melieres, F., Tucholka, P., Zhixiang, W., Zhi-Yuan, C., 1996. A Late Pleistocene-Holocene lacustrine record from Lake Manas, Zunggar northern Xinjiang, western China. Palaeogeography, Palaeoclimatology, Palaeoecology 120, 105-121.
Roos, C.I., Scott, A.C., 2018. A comparison of charcoal reflectance between crown and surface fire contexts in dry south-west USA forests. International Journal of Wildland Fire 27, 396-406.
Roos, C.I., Williamson, G.J., Bowman, D.M.J.S., 2019. Is Anthropogenic Pyrodiversity Invisible in Paleofire Records? Fire 2.
Roos, C.I., Zedeno, M.N., Hollenback, K.L., Erlick, M.M.H., 2018. Indigenous impacts on North American Great Plains fire regimes of the past millennium. Proc Natl Acad Sci U S A 115, 8143-8148.
Rudaya, N., Krivonogov, S.K., Słowiński, M., Cao, X.-y., Zhilich, S., 2020. Postglacial history of the Steppe Altai: Climate, fire and plant diversity. Quaternary Science Reviews 249.
Rudaya, N., Tarasov, P., Dorofeyuk, N., Solovieva, N., Kalugin, I., Andreev, A., Daryin, A., Diekmann, B., Riedel, F., Tserendash, N., 2009. Holocene environments and climate in the Mongolian Altai reconstructed from the Hoton-Nur pollen and diatom records: a step towards better understanding climate dynamics in Central Asia. Quaternary Science Reviews 28, 540-554.
Ryan, R., Dosseto, A., Dlapa, P., Thomas, Z., Simkovic, I., Mooney, S., Bradstock, R., 2025. Using Fourier Transform Infrared spectroscopy to produce high-resolution centennial records of past high-intensity fires from organic-rich sediment deposits. International Journal of Wildland Fire 34.
Ryan, R., Thomas, Z., Simkovic, I., Dlapa, P., Worthy, M., Wasson, R., Bradstock, R., Mooney, S., Haynes, K., Dosseto, A., 2024. Assessing changes in high-intensity fire events in south-eastern Australia using Fourier Transform Infra-red (FITR) spectroscopy. International Journal of Wildland Fire 33.
Schlütz, F., Lehmkuhl, F., 2006. Climatic change in the Russian Altai, southern Siberia, based on palynological and geomorphological results, with implications for climatic teleconnections and human history since the middle Holocene. Vegetation History and Archaeobotany 16, 101-118.
Schmid, M.M.E., Dugmore, A.J., Foresta, L., Newton, A.J., Vésteinsson, O., Wood, R., 2018. How 14C dates on wood charcoal increase precision when dating colonization: The examples of Iceland and Polynesia. Quaternary Geochronology 48, 64-71.
Shi, Y., Shen, Y., Kang, E., Li, D., Ding, Y., Zhang, G., Hu, R., 2007. Recent and Future Climate Change in Northwest China. Climatic Change 80, 379-393.
Tang, X.-l., Lv, X., He, Y., 2013. Features of climate change and their effects on glacier snow melting in Xinjiang, China. Comptes Rendus. Géoscience 345, 93-100.
Théry-Parisot, I., Chabal, L., Chrzavzez, J., Anthracology and taphonomy, from wood gathering to charcoal analysis. A review of the taphonomic processes modifying charcoal assemblages, in archaeologica lcontexts. Palaeogeography, Palaeoclimatology, Palaeoecology 291, 142-153.
Tilman, D., Balzer, C., Hill, J., Befort, B.L., 2011. Global food demand and the sustainable intensification of agriculture. Proceedings of the National Academy of Sciences 108, 20260-20264.
Tinner, W., Hofstetter, S., Zeugin, F., Conedera, M., Wohlgemuth, T., Zimmermann, L., Zweifel, R., 2006. Long-distance transport of macroscopic charcoal by an intensive crown fire in the Swiss Alps - implications for fire history reconstruction. The Holocene 16, 287-292.
Turner, R., Roberts, N., Jones, M.D., 2008. Climatic pacing of Mediterranean fire histories from lake sedimentary microcharcoal. Global and Planetary Change 63, 317-324.
Vachula, R.S., Russell, J.M., Huang, Y., Richter, N., 2018. Assessing the spatial fidelity of sedimentary charcoal size fractions as fire history proxies with a high-resolution sediment record and historical data. Palaeogeography, Palaeoclimatology, Palaeoecology 508, 166-175.

Walsh, M., Dotte-Sarout, E., Brady, L.M., Bradley, J., Ash, J., Wesley, D., Evans, S., Barrett, D., 2024. Collaborative anthracology and cultural understandings of wood charcoal in Marra Country (northern Australia). Archaeological and Anthropological Sciences 16.
Wang, D., Guan, D., Zhu, S., Kinnon, M.M., Geng, G., Zhang, Q., Zheng, H., Lei, T., Shao, S., Gong, P., Davis, S.J., 2020. Economic footprint of California wildfires in 2018. Nature Sustainability 4, 252-260.
Whitlock, C., Larsen, C., 2001. Charcoal as a fire proxy, in: Smol, J.P., Birks, H.J.B.,, Last, W.M. (Eds.), Tracking Environmental Change Using Lake Sediments. Terrestrial, Algal, and Siliceous Indicators. Kluwer, Dordrecht, The Netherlands, pp. 75-97.
Wood, R., King, F., Esmay, R., Chen, Q., Schneider, L., Dotte-Sarout, E., Fallon, S., Fryirs, K., Gillespie, R., Blong, R., 2023. The Size Inherited Age Effect on Radiocarbon Dates of Alluvial Deposits: Redating Charcoal Fragments in a Sand-Bed Stream, Macdonald River, Nsw, Australia. Radiocarbon 66, 1006-1019.
Xu, C., Li, J., Zhao, J., Gao, S., Chen, Y., 2015. Climate variations in northern Xinjiang of China over the past 50 years under global warming. Quaternary International 358, 83-92.
Zhang, D., Chen, X., Li, Y., Zhang, S., 2020. Holocene vegetation dynamics and associated climate changes in the Altai Mountains of the Arid Central Asia. Palaeogeography, Palaeoclimatology, Palaeoecology 550.
Zhang, Y., Meyers, P.A., Liu, X., Wang, G., Ma, X., Li, X., Yuan, Y., Wen, B., 2016. Holocene climate changes in the central Asia mountain region inferred from a peat sequence from the Altai Mountains, Xinjiang, northwestern China. Quaternary Science Reviews 152, 19-30.
Zhu, X., Zhang, M., Wang, S., Qiang, F., Zeng, T., Ren, Z., Dong, L., 2015. Comparison of monthly precipitation derived from high-resolution gridded datasets in arid Xinjiang, central Asia. Quaternary International 358, 160-170.

Figure 1. A) GoogleEarth image (Image: Landsat/Copernicus) showing Aksay Pond (red star) and sites discussed in the text. Inset shows the region of interest in relation to national borders in central Asia. B) Southward photo of Aksay Pond showing the displaced shutter ridge, fault scarp and trench A and B locations. C) Photo composite of Trench A north face. D) Stratigraphic interpretation of C) with ^{14}C AMS charcoal sites. E) Photo composite of Trench B south face. F) Stratigraphic interpretation of E) with ^{14}C AMS charcoal sites from both trench faces in their equivalent stratigraphic position.

Figure 2. Calibrated $F^{14}C$ and ^{14}C posterior distributions showing the age range of each charcoal date recovered from Aksay Pond. The individual dates are grouped into three phases, Phase 3 (pink dates but contains the three $F^{14}C$ dates that are removed from subsequent analysis), Phase 2 (blue dates) and Phase 1 (orange dates). Vertical bars at the earlier and later extremities of the calibrated ^{14}C posterior distributions are the start and end dates of the three phases. Also shown are colour-coded horizontal bars that represent the 95% HPD ranges of all of the dates within a phase.

Figure 3. Plot of the full posterior distributions of each of the three phases of ^{14}C ages (colours as per Fig. 2) showing the statistically significant periods of hiatus (vertical pale blue bars).

Figure 4. Plot showing the full posterior distribution of each phase of burning recorded from Aksay Pond (Phases 1 to 3) and other studies from the Altai Ranges, including burning peaks identified by Olivier et al. (2003) and the burning peak and minimum identified by Eichler et al. (2011).

Table 1: 95% HDP calibrated age range of each charcoal-derived ^{14}C AMS dates extracted from the sedimentary faces at Aksay Pond.

Name	Lab code	Sample material	Trench[1]	Depth (cm)	^{14}C age (yrs BP)	$\delta^{13}C$ relative to VPDB	Radioactivity ($F^{14}C$)	Calibrated modern age range (year CE 2s)	95% HPD low (CE)	95% HPD high (CE)	Mean (CE)	HPD total %	Phase	Sample No in Fig 1
FU12-C14-51	SUERC-53136 (GU34157)	Charcoal	BS	100	Post 1950	-26.7	1.1754 ± 0.0034	1959-1989	1959	1989	1988	95	Phase 3	12
FU12-C14-81	SUERC-48692 (GU31575)	Charcoal	BS	54	Post 1950	-21.2	1.2178 ± 0.0038	1959-1985	1959	1985	1987	95	Phase 3	21
FU12-C14-94	SUERC-48696 (GU31577)	Charcoal	BS	100	Post 1950	-26.2	1.5340 ± 0.0048	1970-1972	1970	1972	1971	95	Phase 3	22
FU12-C14-04	SUERC-46558 (GU30430)	Charcoal	AN	105	70 ± 34	-21.6		1690-1921	1690	1921	1821	95	Phase 3	1
FU12-C14-05	SUERC-46559 (GU30431)	Charcoal	AN	210	56 ± 34	-23.9		1688-1924	1688	1924	1821	95	Phase 3	2
FU12-C14-08	SUERC-46560 (GU30432)	Charcoal	AN	30	420 ± 34	-24.6		1673-1942	1673	1942	1817	95	Phase 3	3
FU12-C14-10	SUERC-46561 (GU30434)	Charcoal	AN	205	68 ± 34	-25.8		1673-1942	1673	1942	1816	95	Phase 3	4
FU12-C14-18	SUERC-46563 (GU30438)	Charcoal	AN	195	142 ± 34	-23.2		1679-1941	1679	1941	1819	95	Phase 3	8

FU12-C14-123	SUERC-46581 (GU30463)	Charcoal	AN	10	220 ± 34	-20.7		1672-1943	1672	1943	1813	94.5	Phase 3	10
FU12-C14-19	SUERC-53132 (GU34155)	Charcoal	AN	28	128 ± 26	-24.1		1670-1945	1670	1945	1811	95	Phase 3	11
FU12-C14-46	SUERC-46570 (GU30442)	Charcoal	BS	165	127 ± 34	-25.5		1669-1947	1669	1947	1809	95	Phase 3	14
FU12-C14-44	SUERC-46569 (GU30441)	Charcoal	BS	199	148 ± 34	-28.1		1668-1948	1668	1948	1809	95	Phase 3	16
FU12-C14-41	SUERC-48687 (GU31569)	Charcoal	BS	235	842 ± 26	-25		1668-1950	1668	1950	1808	95	Phase 3	17
FU12-C14-39	SUERC-46567 (GU30439)	Charcoal	BS	260	848 ± 34	-22.5		1659-1950	1659	1950	1796	95	Phase 3	18
FU12-C14-40	SUERC-46568 (GU30440)	Charcoal	BS	277	145 ± 34	-24.1		1662-1950	1662	1950	1791	95	Phase 3	19
FU12-C14-74	SUERC-48691 (GU31573)	Charcoal	BS	58	172 ± 23	-21.1		1654-1950	1654	1950	1792	95	Phase 3	20
FU12-C14-69	SUERC-53137 (GU34159)	Charcoal	BS	180	729 ± 29	-24.5		1530-1950	1530	1950	1753	95	Phase 3	23
FU12-C14-55	SUERC-46571 (GU30445)	Charcoal	BN	150	77 ± 34	-26.5		1693-1918	1693	1918	1820	95	Phase 3	25
FU12-C14-57	SUERC-46572 (GU30446)	Charcoal	BN	230	123 ± 34	-26.8		1691-1921	1691	1921	1821	95	Phase 3	26
FU12-C14-60	SUERC-46573 (GU30447)	Charcoal	BN	53	332 ± 34	-27.3		1476-1641	1476	1641	1559	95	Phase 2	27
FU12-	SUERC-46577	Charcoal	BN	58	135 ± 34	-24.6		1425-	1425	1621	1485	95	Phas	28

C14-66	(GU30449)							1621					e 2	
FU12-C14-73	SUERC-46578 (GU30451)	Charcoal	BN	76	171 ± 34	-23.7		1053-1268	1053	1268	1199	95	Phase 1	29
FU12-C14-104	SUERC-46579 (GU30459)	Charcoal	BN	147	179 ± 34	-26.6		1165-1262	1165	1262	1210	95	Phase 1	30
FU12-C14-112	SUERC-46580 (GU30460)	Charcoal	BN	36	146 ± 34	-26.7		1229-1378	1229	1378	1281	95	Phase 1	31

[1] Trench codification is A = Trench A, B = Trench B, N = North Face, S= South Face

Table 2. 95% HPD results of the Bayesian phase duration and gap analyses for the three charcoal ^{14}C phases identified from Aksay Pond.

	Phase	Start Year (CE)	End Year (CE)	Duration (yrs)
Phase Duration Analysis	Phase 3	1724	1900	177
	Phase 2	1415	1646	231
	Phase 1	1176	1287	111
Gap Analysis	Phase 3 & Phase 2	1637	1715	78
	Phase 1 & Phase 2	1290	1421	131

Table 3. 95% HPD results of the Bayesian phase duration and gap analyses for the three charcoal ^{14}C phases identified from Aksay Pond, the three burning phases identified by Olivier et al. (2006) and the burning minimum and peak identified by Eichler et al. (2011).

	Phase	Start Year (CE)	End Year (CE)	Duration (yrs)
Phase Duration Analysis	Olivier Peak 1	1888	1964	76
	Olivier Peak 2	1864	1916	52
	Olivier Peak 3	1852	1878	26
	Phase 3	1719	1894	176
	Eichler Minima	1574	2020	446
	Eichler Peak	1538	1748	209
	Phase 2	1416	1646	230
	Phase 1	1178	1290	111
Gap Analysis	Olivier Peak 1 & Olivier Peak 2	NA	NA	NA
	Olivier Peak 1 & Olivier Peak 3	1882	1892	10
	Phase 3 & Olivier Peak 1	NA	NA	NA
	Phase 3 & Olivier Peak 2	NA	NA	NA

	Phase 3 & Olivier Peak 3	NA	NA	NA
	Phase 3 & Eichler Peak	NA	NA	NA
	Phase 3 & Eichler Minimum	NA	NA	NA
	Eichler Minimum & Eichler Peak	NA	NA	NA
	Phase 2 & Phase 3	1636	1715	79
	Phase 2 & Eichler Minimum	NA	NA	NA
	Phase 2 & Eichler Peak	NA	NA	NA
	Phase 1 & Phase 2	1292	1422	130
	Phase 1 & Eichler Peak	1297	1560	263
	Phase 1 & Eichler Minimum	1306	1562	256

Declaration of interests

☒ The authors declare that they have no known competing financial interests or personal relationships that could have appeared to influence the work reported in this paper.

☐ The authors declare the following financial interests/personal relationships which may be considered as potential competing interests:

Highlights:

- ^{14}C AMS charcoal dating defines the fire history of the southern Altai Range
- Three periods of burning occurred at *ca.* 1170-1290, 1410-1650 CE and 1720-1900 CE
- Bayesian statistics demonstrates complex spatial burning history across the Altai Range